Electronic Supplementary Information

High-Performance Ladder-type Conjugated Polymer/Carbon Nanotube Nanocomposites Blended with Elastomer for Stretchable Thermoelectric Thin Films

Qing-Bao Zheng,[a]‡ Chi-Chun Tseng,[b]‡ Meng-Hao Lin,[a] Jhih-Min Lin,[c] Shih-Huang Tung,[d] Yen-Ju Cheng[b,e] and Cheng-Liang Liu*[a,f]*

a. Department of Materials Science and Engineering, National Taiwan University, Taipei 10617, Taiwan. E-mail: liucl@ntu.edu.tw

b. Department of Applied Chemistry, National Yang Ming Chiao Tung University, Hsinchu 30010, Taiwan. E-mail: yjcheng@nycu.edu.tw

c. National Synchrotron Radiation Research Center, Hsinchu 30076, Taiwan.

d. Institute of Polymer Science and Engineering, National Taiwan University, Taipei 10617, Taiwan.

e. Center for Emergent Functional Matter Science, National Yang Ming Chiao Tung University, Hsinchu 30010, Taiwan.

f. Advanced Research Center for Green Materials Science and Technology, National Taiwan University, Taipei 10617, Taiwan.

‡ These Authors Contributed equally to this work.

Characterization

The geometries and energy levels of the polymers were modeled via density-functional theory (DFT) calculations at the B3LYP/6-311G** level by using the Gaussian software. The electrical conductivities and Seebeck coefficients of the various composites were measured by commercial ZEM-3 measurement system (ADVANCE RIKO Inc., Japan). Prior to measurement, silver paste contacts were strategically applied to both ends of the samples to minimize electrode contact resistance. These measurements were conducted within a helium environment at reduced pressure and a temperature of 303 K, employing three distinct temperature gradients. To explore the π–π interfacial interactions between the various TPT-based conjugated polymers and the CNTs, the ultraviolet-visible (UV-vis) absorption spectra of the samples with and without CNTs were acquired on a (Hitachi U-4100). In addition, the solution photoluminescence (PL) spectra were obtained using a Horiba Jobin Yvon Fluorolog-3 Spectrofluorometer. The PL quenching efficiency (PLQE) was obtained from the PL results by using the formula:

$$\text{PLQE (\%)} = (I_0 - I/I_0) \times 100\% \quad \text{(S1)}$$

where I_0 and I are the PL peak intensities of the nanocomposites without and with CNTs, respectively. The structural characteristics were further elucidated by Raman spectroscopy (Horiba Jobin Yvon LabRAM HR800 UV spectrometer) at an excitation wavelength of 532 nm, which resonates with the CNTs and coincides with the absorbance of the conjugated polymers. In addition, ultraviolet photoemission spectroscopy (UPS) measurements were conducted by a PHI 5000 VersaProbe Ш (ULVAC-PHI. Inc). The surface morphologies of the nanocomposite films were examined by scanning electron microscopy (SEM; JEOL JSM-7600F), atomic force microscopy (AFM; Hitachi AFM 5100N), and transmission electron microscopy (TEM; JEOL JEM-2100F). AFM studies of thin films were performed at tapping mode under ambient conditions using Hitachi SI-DF3PS tips with a resonant frequency = 70 kHz and force constant = 2.0 N m^{-1}. For the TEM analysis, the samples were diluted and coated onto copper grids. In addition, grazing-incidence wide-angle X-ray scattering (GIWAXS) patterns were obtained at the TPS 25A beamlines at National Synchrotron Radiation Research Center (NSRRC, Taiwan) and used to examine the microstructures of the various nanocomposites. Further, the elastic moduli of the various polymer/CNT/SEBS films were evaluated via a Derjanguin-Muller-Toporov (DMT) contact mechanics model analysis of the AFM images.

Table S1 Molecular weights, polydispersity index, and thermal properties of TPT-based conjugated polymers.

	M_n [a]	M_w [b]	PDI [c]	T_d [d] (℃)	T_g [e] (℃)
TPT-TPD	34000	90000	2.64	430	133
TPT-QX	28000	72000	2.58	427	141
TPT-TT	29000	63000	2.18	421	113

[a] M_n = number-average molar mass

[b] M_w = weight-average molar mass

[c] PDI = polydispersity index

[d] T_d = decomposition temperature estimated by the 5% weight loss.

[e] T_g = glass transition temperature

Table S2 Hall effect measurement of three TPT-based conjugated polymer/CNT nanocomposite films.

nanocomposite	carrier concentration $[cm^{-3}] \times 10^{22}$	μ $[cm^2\,V^{-1}\,s^{-1}]$
TPT-TPD/CNT	2.41	0.18
TPT-QX/CNT	2.25	0.21
TPT-TT/CNT	2.34	0.37

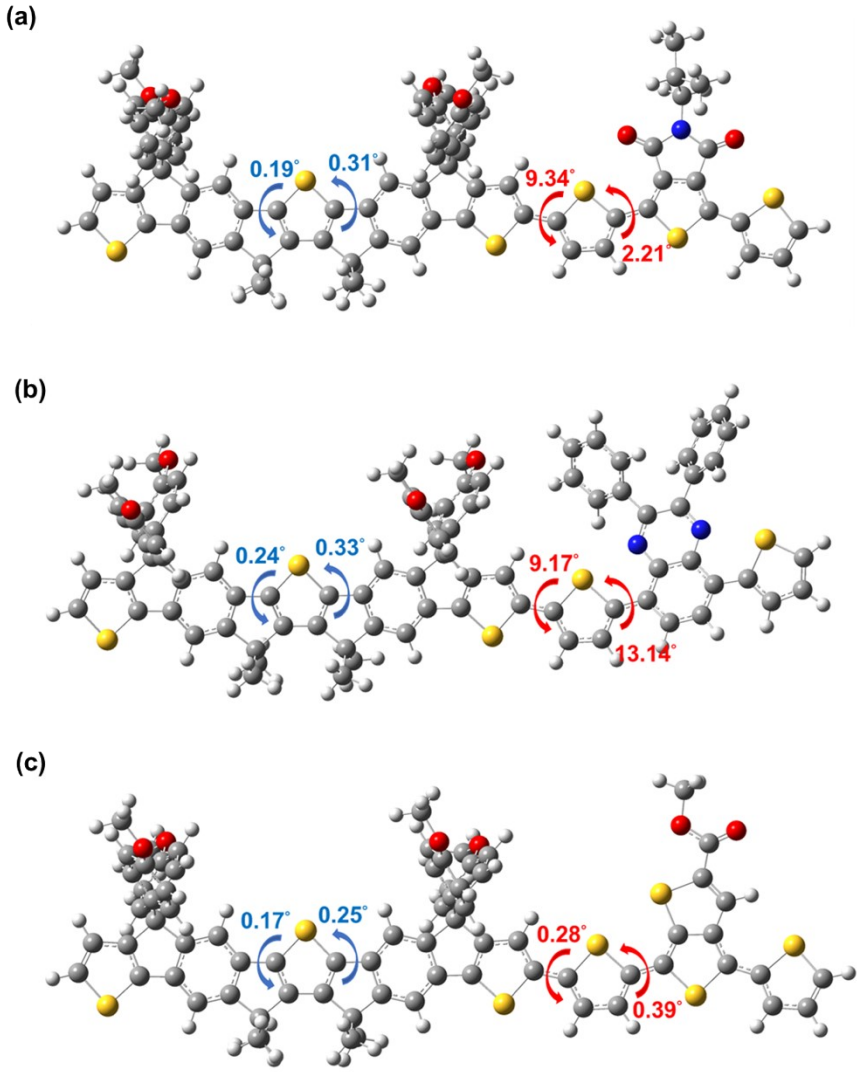

Fig. S1 Top view of three TPT-based conjugated polymer (a) TPT-TPD, (b) TPT-QX, and (c) TPT-TT from DFT calculation results.

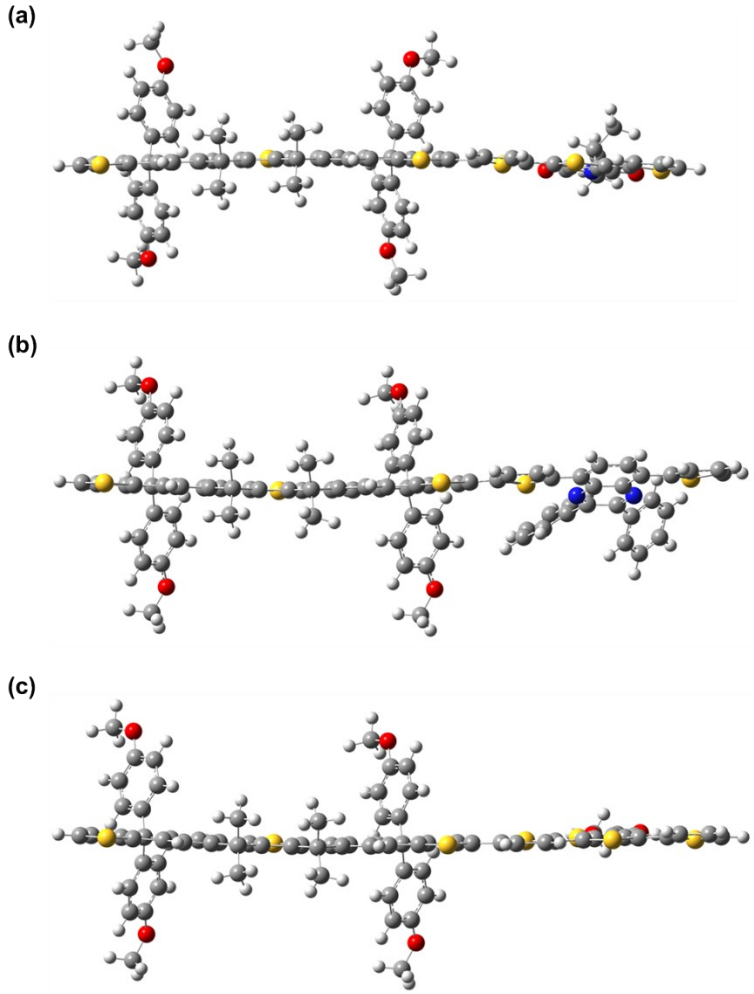

Fig. S2 Side view of three TPT-based conjugated polymer (a) TPT-TPD, (b) TPT-QX, and (c) TPT-TT from DFT calculation results.

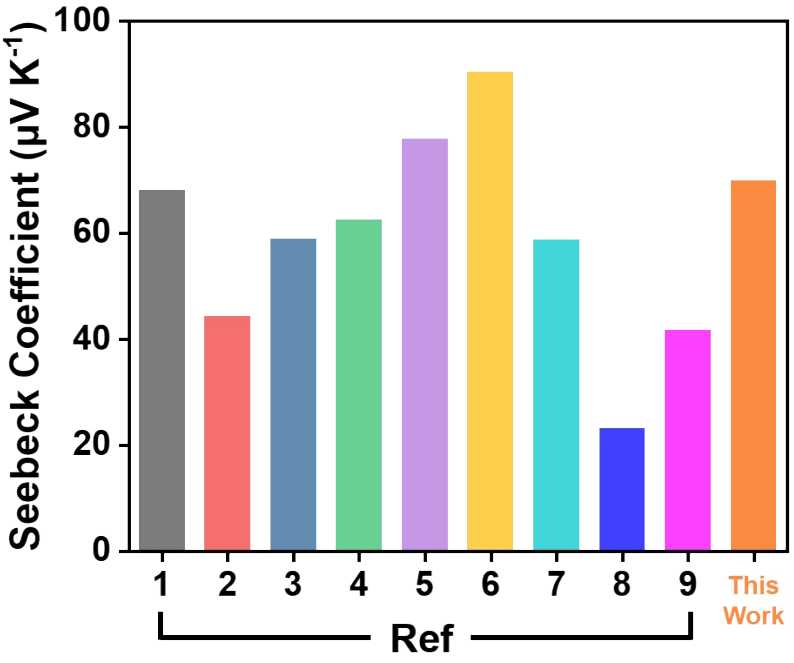

Fig. S3 Comparison of Seebeck coefficient between the conjugated polymer/CNT nanocomposites investigated in this work and those reported in recent literature.[1-9]

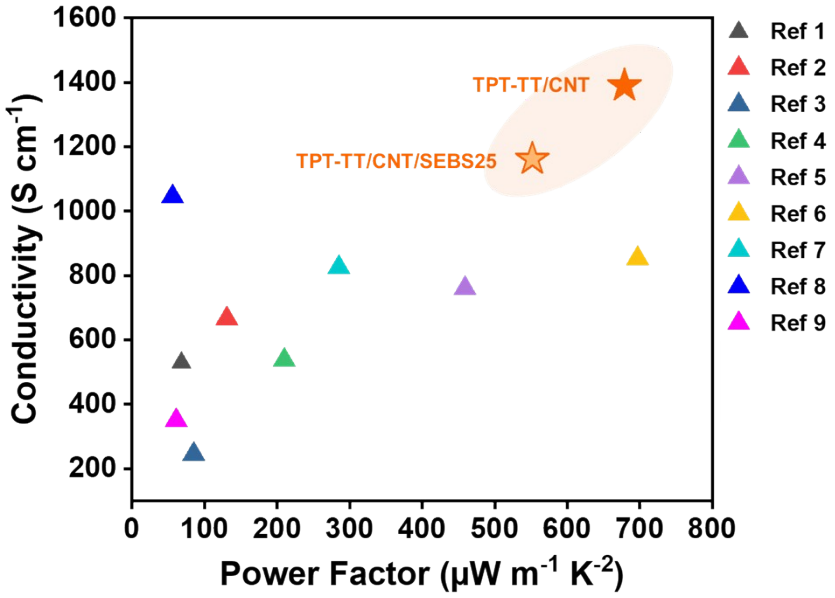

Fig. S4 Comparison of PF values between the conjugated polymer/CNT nanocomposites investigated in this work and those reported in recent literature.[1-9]

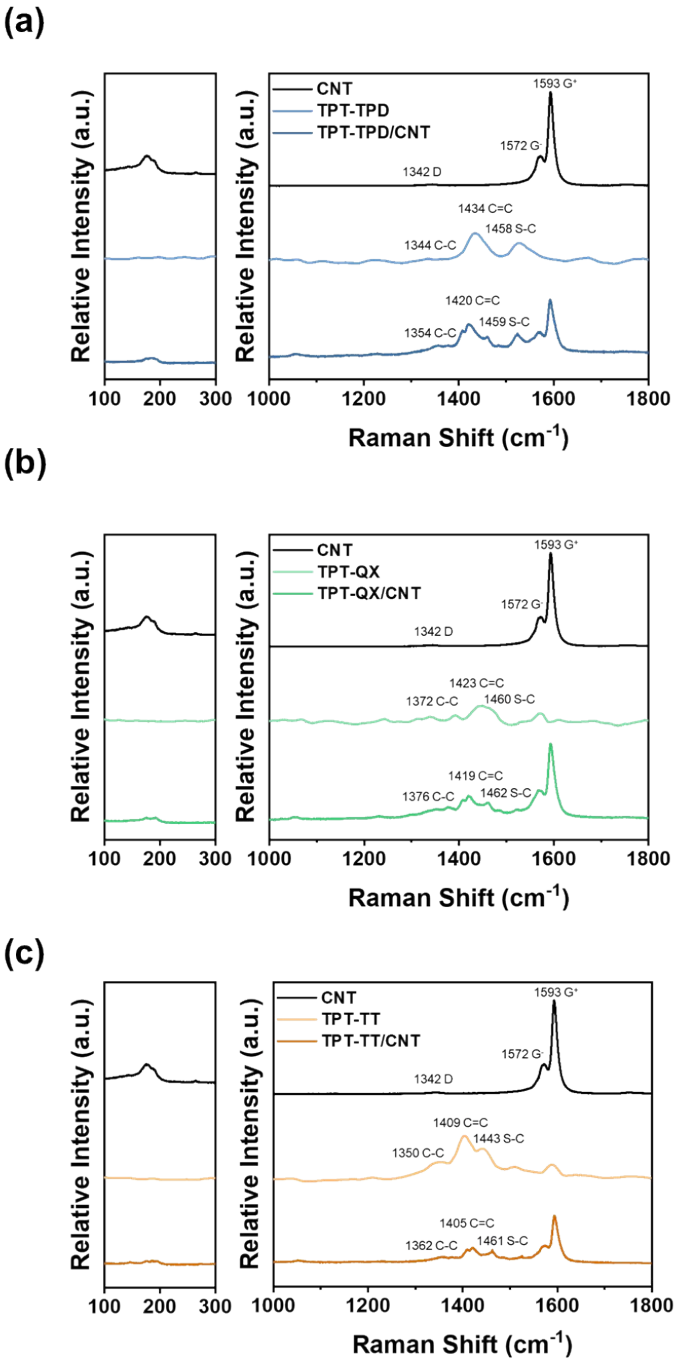

Fig. S5 Raman spectra of the pristine CNT and (a) TPT-TPD and TPT-TPD/CNT, (b) TPT-QX and TPT-QX/CNT, (c)TPT-TT and TPT-TT/CNT.

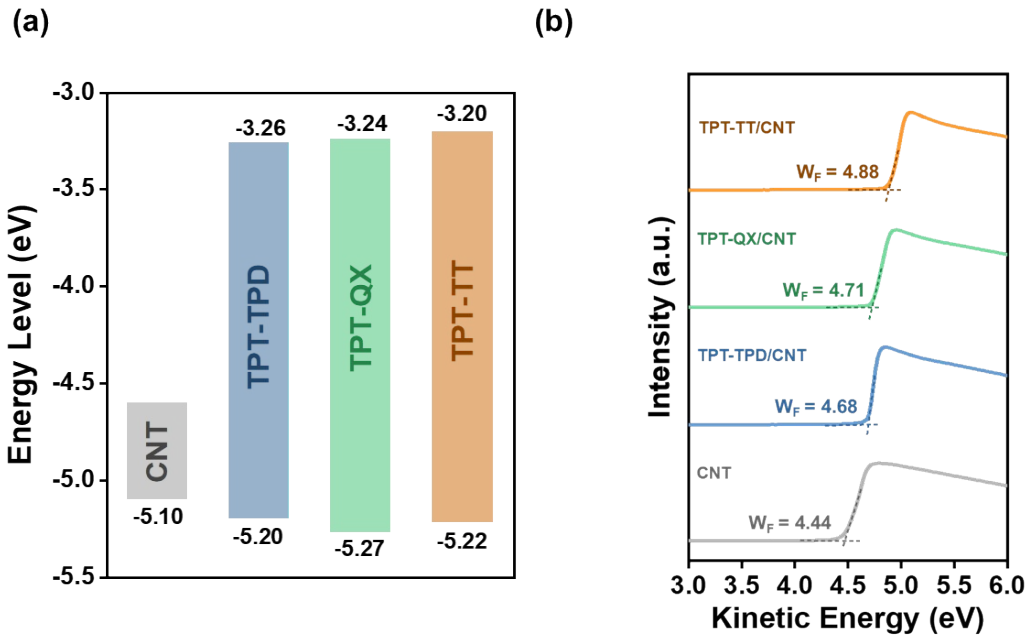

Fig. S6 (a) Energy diagrams of studied TPT-based conjugated polymers and CNT. (b) UPS spectra for the secondary electron cut-off region and work function for TPT-based conjugated polymer/CNT nanocomposite films compared to pristine CNT films.

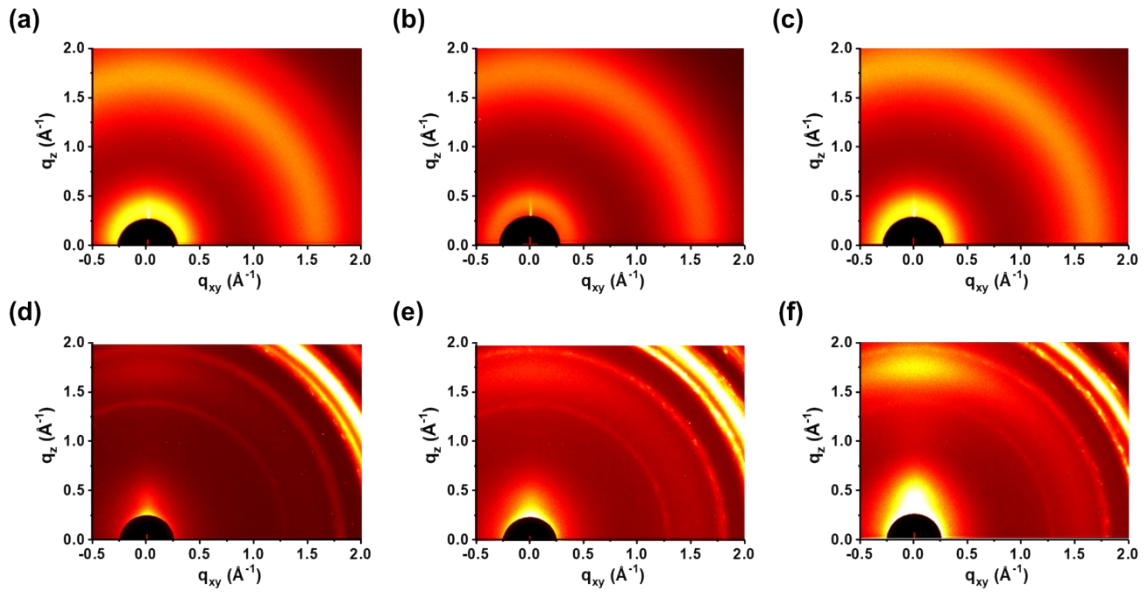

Fig. S7 2D GIWAXS profiles of the pristine (a) TPT-TPD and (d) TPT-TPD/CNT; (b) TPT-QX and (e) TPT-QX/CNT; (c) TPT-TT and (f) TPT-TT/CNT films.

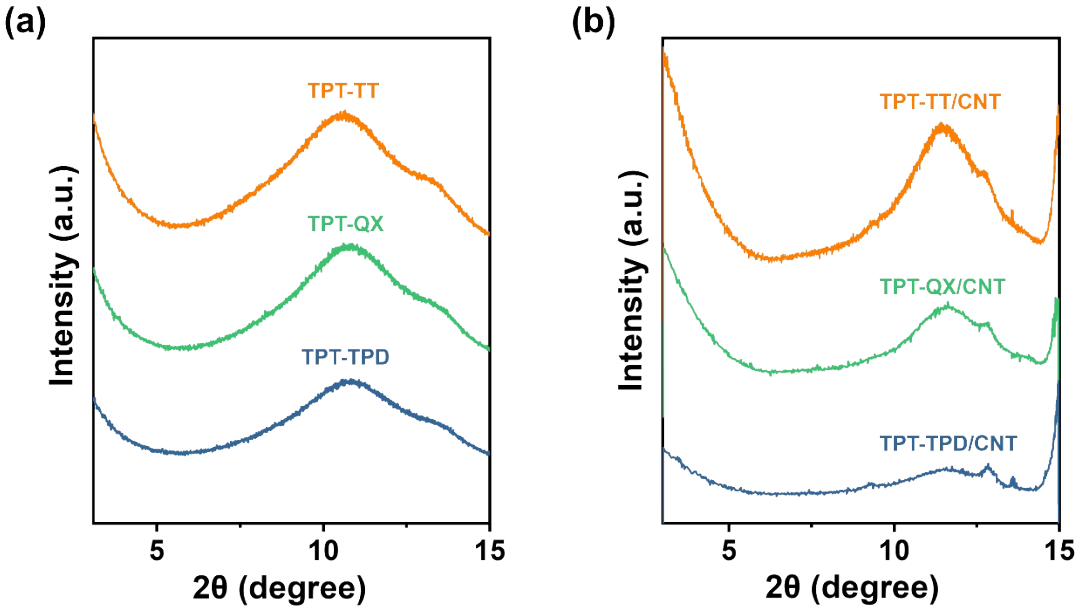

Fig. S8 1D GIWAXS profiles of the (a) TPT-based conjugated polymers and (b) their corresponding TPT-based conjugated polymers/CNT nanocomposite films.

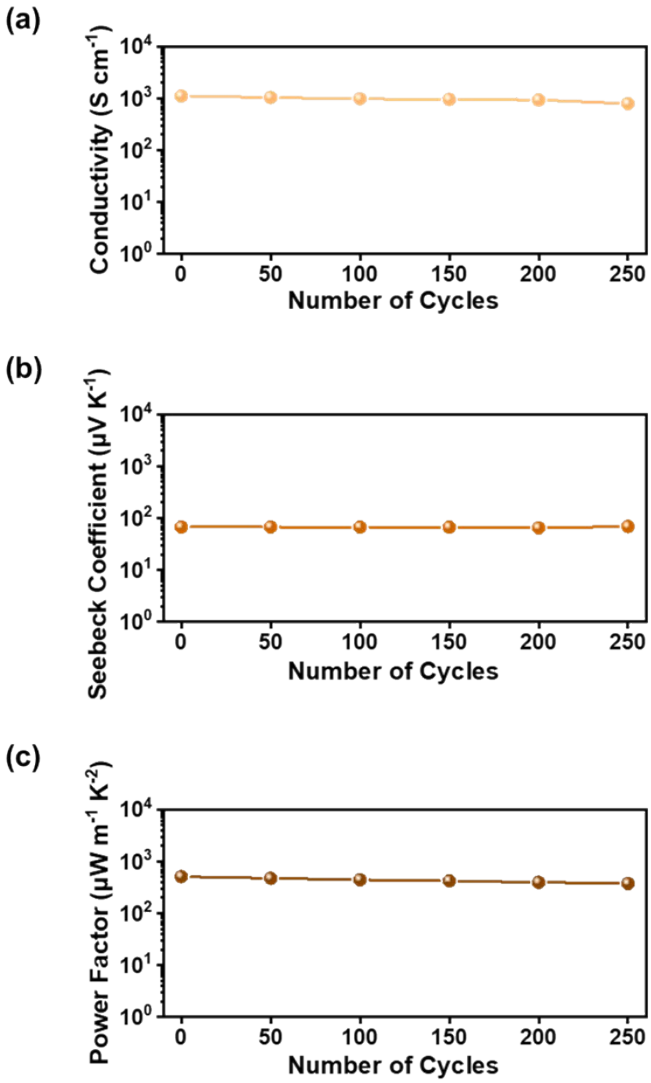

Fig. S9 Endurance of (a) conductivity, (b) Seebeck coefficient and (c) PF of TPT-TT/CNT/SEBS25 ternary nanocomposite films subjected to 25% strain after 250 stretch/release cycles.

Reference

1. L. Wang, C. Pan, Z. Chen, W. Zhou, C. Gao and L. Wang, *ACS Appl. Energy Mater.*, 2018, **1**, 5075.
2. T. Wan, X. Yin, C. Pan, D. Liu, X. Zhou, C. Gao, W. Y. Wong and L. Wang, *Polymer*, 2019, **11**, 593.
3. H. Zhou, X. Li, C. Gao, F. Yang, X. Ye, Y. Liu and L. Wang, *Compos. Sci. Technol.*, 2021, **201**, 108518.
4. Y. H. Kang, U.-H. Lee, I. H. Jung, S. C. Yoon and S. Y. Cho, *ACS Appl. Electron. Mater.*, 2019, **1**, 1282.
5. J. Jung, E. H. Suh, Y. J. Jeong, H. S. Yang, T. Lee and J. Jang, *ACS Appl. Mater. Interfaces*, 2019, **11**, 47330.
6. S. H. Kim, S. Jeong, D. Kim, C. Y. Son and K. Cho, *Adv. Electron. Mater.*, 2023, **9**, 2210293.
7. H. Huang, Z. Chen, X. Chen, J. Jin, S. Huang, D. Wang, L. Wang and D. Liu, *Adv. Mater. Interfaces*, 2022, **9**, 2201193.
8. Z. Chen, M. Lai, L. Cai, W. Zhou, D. Xie, C. Pan and Y. Qiu, *Polymer*, 2020, **12**, 1447.
9. X. Zhou, C. Pan, A. Liang, L. Wang and W.-Y. Wong, *Compos. Sci. Technol.*, 2017, **145**, 40.